Supplementary information

Quasi-dynamic study on electrochemical properties of O3-high-Ni ternary single-crystal cathode materials with mirror symmetry: a first-principles study

Naigen Zhou,[a] Yazhou Wang, *[a] and Hong Cui*[b]

Design ideas for the single layer of NCM811 structure

High-nickel ternary cathode materials can be regarded as solid solutions of $LiCoO_2$, $LiNiO_2$, $LiMnO_2$, which belong to the O3-type phase. The $LiNi_{0.8}Co_{0.1}Mn_{0.1}O_2$(NCM811) crystal structure was modelled based on α-$NaFeO_2$ phase $Li_3Co_3O_6$ in a stoichiometric ratio of Ni : Co : Mn=8:1:1.

Firstly, a 4×5×1 supercell was constructed based on O3-TYPE $LiCoO_2$ primary cells, and then occupation design was carried out by taking into account the distances between Ni, Co, Mn. In order to construct all models as possible, the study will be carried out with a single TM layer which will be further extended to the bulk structure model. Since Ni has the highest concentration, the main consideration is the variation of the location of Co and Mn atoms. As shown in Fig. S1, five scenarios of Co and Mn occupancy were designed in the monolayer structure (labelled as green rhombus).

Many studies have shown that the uniform dispersion of transition metal atoms in the crystal structure satisfies the need to maintain the chemical homogeneity required for stable chemical reactions.[1-3] Therefore, the structures corresponding to I III, IV are not favorable for the stability of the electrode materials involved in chemical reactions. After obtaining the monolayer structure, the possible locations of Co, Mn atoms in the monolayer structure were designed and labelled as a, a', b, b', c, c'(in Fig. S1), respectively. In these, the rhombic structure composed of Co and Mn atoms in a, a' has rotational symmetry, and the rhombic structure composed of Co and Mn atoms in c, c' has mirror symmetry. As a result, there is no significant polarisation of the crystal structure. However, the b, b' structure is significantly polarised, which is disadvantageous for structural stability.[4] In the end, four excellent single TM layer structures (a, a', c, c') are obtained.

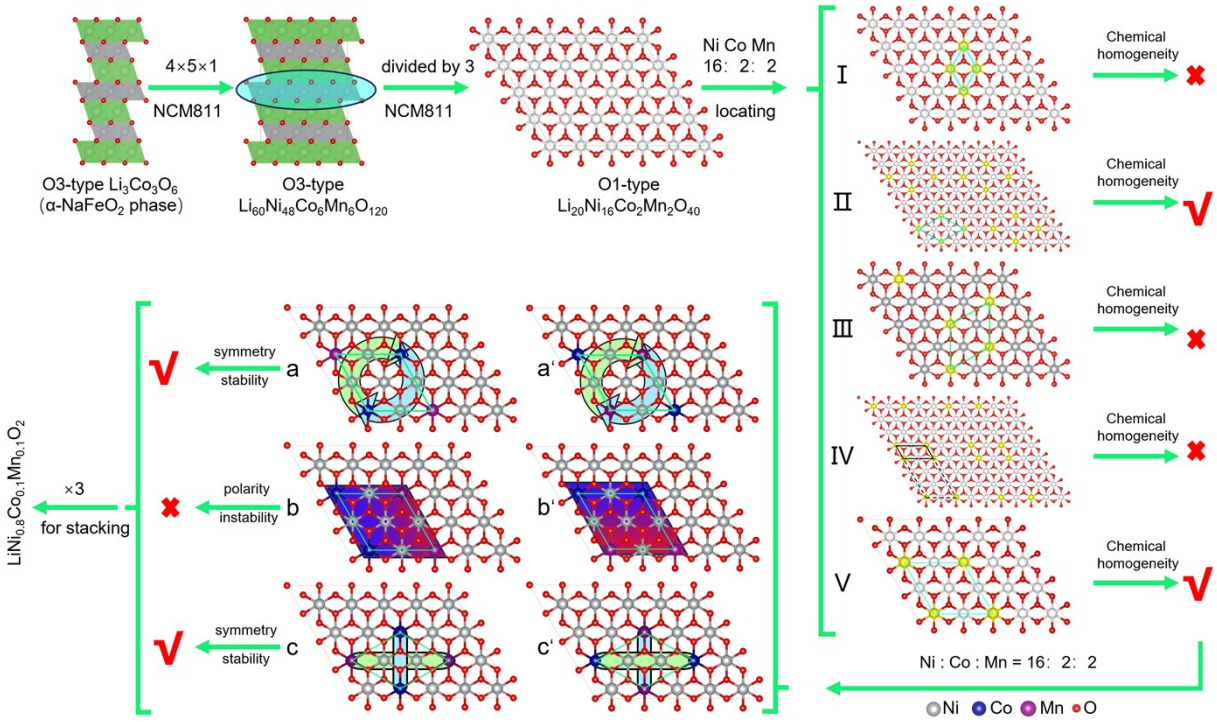

Fig. S1. Transition metal layer structure design ideas for layered transition metal oxide NCM811. The grey, blue, and purple spheres represent Ni, Co, and Mn atoms, respectively.

Bulk structure

O3-type NCM811 was structured based on the designed monolayer structure. It is shown that the structure with high symmetry has lower energy and ultra-high electronic conductivity compared to other counterparts, which helps to maintain the structural stability of the cathode material as well as the ultra-high conductivity.[5-6] As shown in Fig. S2, 16 NCM811 structures with mirror symmetry were designed.

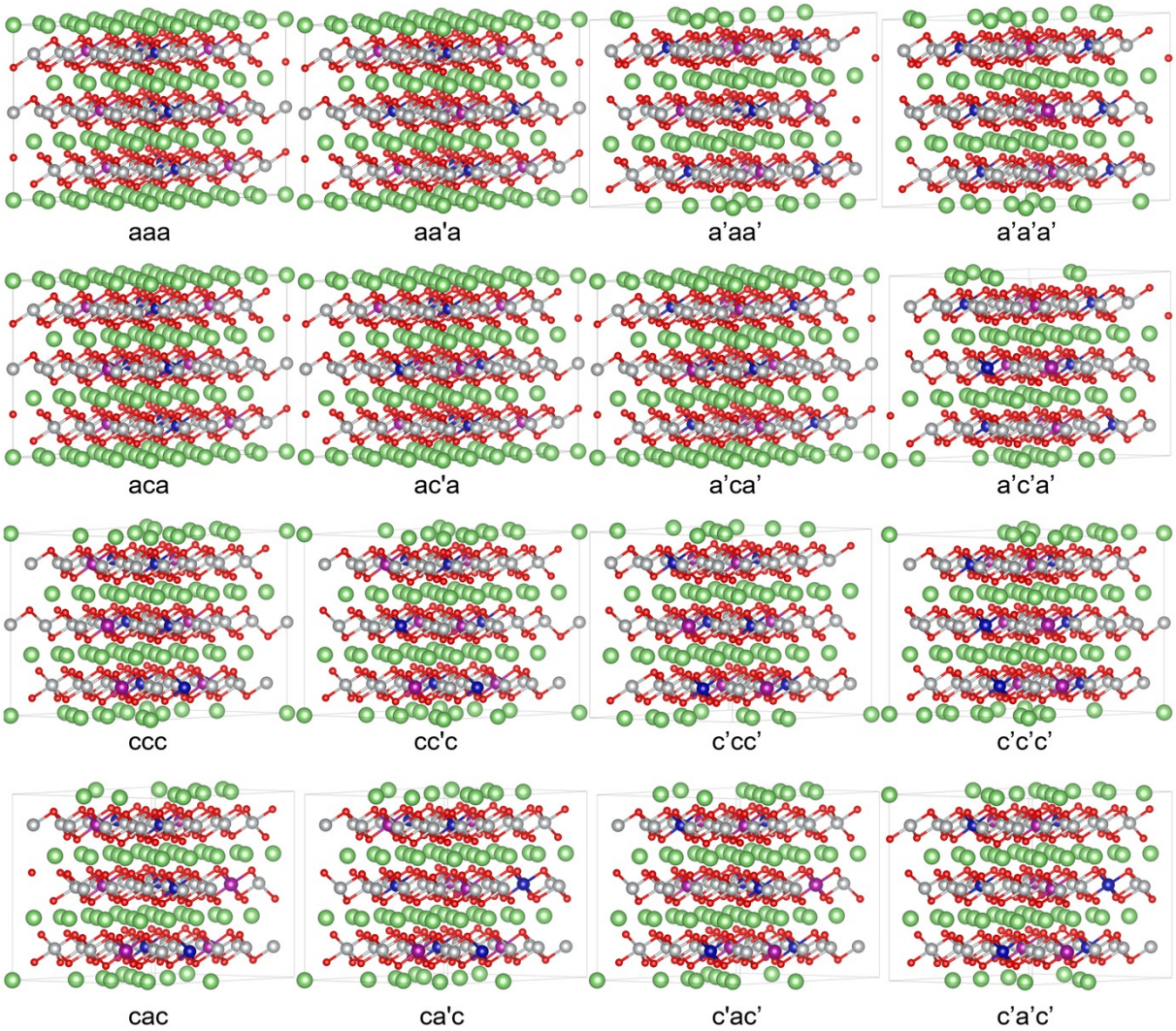

Fig. S2. 16 types of NCM811 with O3-type structures. ' denotes that the Co/Mn atomic locations were exchanged. The green, grey, blue, purple and red spheres represent Li, Ni, Co, Mn and O atoms respectively.

Anatomy of bulk structure

The spin DFT was used to calculate the total energy and magnetizations of the 16 structures designed, as shown in Fig. S3(a). The energies of the 16 structures designed are -1262.95 eV, -1263.97 eV, -1263.3 eV, -1261.25 eV, -1262.4 eV, -1263.17 eV, -1261.85 eV, -1262.23 eV, -1263.59 eV, -1262.57 eV, -1263.54 eV, -1263.65 eV, -1263.66 eV, -1263.52 eV, -1263.77 eV, -1261.81 eV, respectively. Magnetizations fluctuate between 51.13 μB and 76 μB, which indicates that all structures are paramagnetic crystals. Fig. S3(b) shows a mirror symmetry schematic of the aa'a structure. The mirror symmetry schematic of the aa'a structure is

shown in Fig. S3(b), where quasi-perfect symmetry is introduced in the crystal structure.

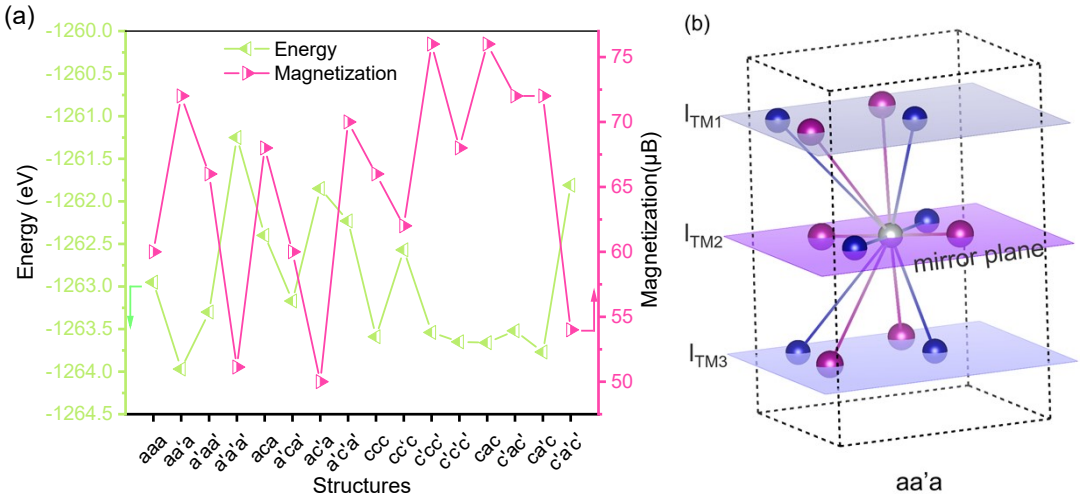

Fig. S3 (a) Total energy and magnetization of the 16 structures. (b) aa'a Mirror Symmetry Schematics. The l_{TM1} and l_{TM3} are mirror images of each other with l_{TM2} as the mirror plane.

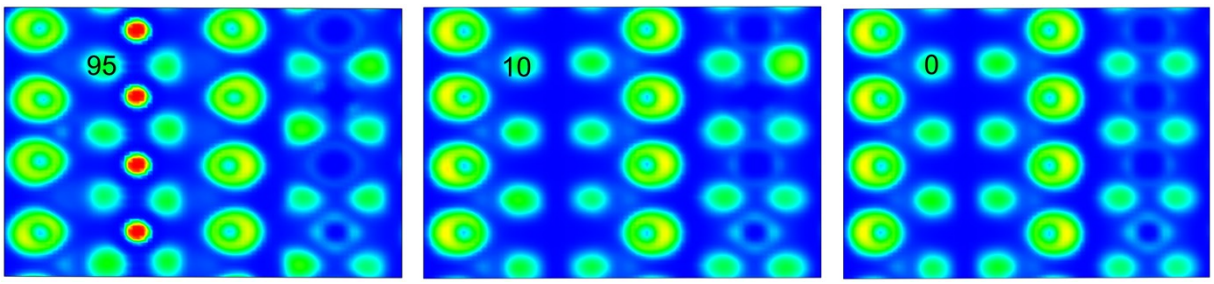

Fig. S4. NCM811 lectron local projections of different SOC states. The blackbody index represents the Li content of the structure.

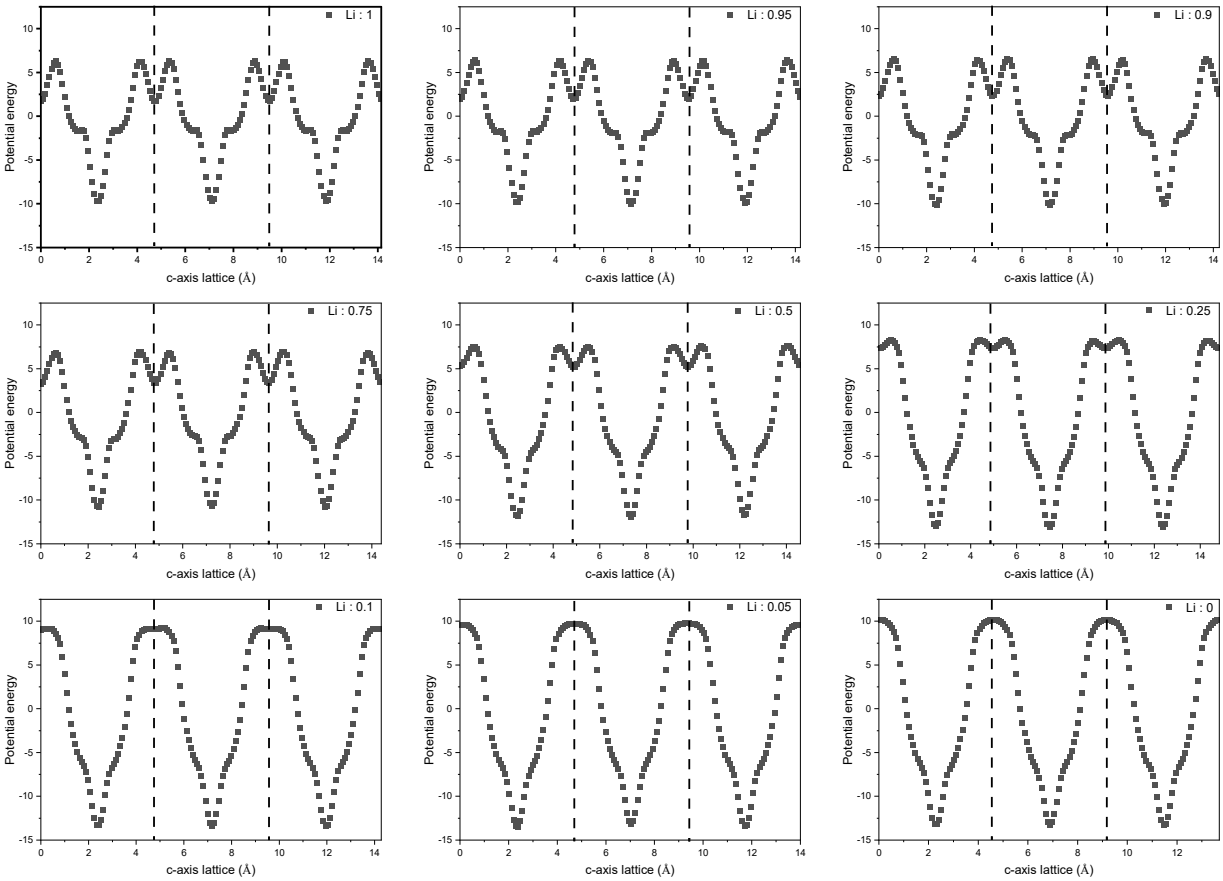

Fig. S5. Plane average value (along [001]) of the total potential energy for different charging states. The black dashed line represents the potential energy of Li.

Tab. S1. O atoms Bader charge in structures with different Li concentrations

atoms	Li : 1	Li : 0.95	Li : 0.9	Li : 0.75	Li : 0.5	Li : 0.25	Li : 0.1	Li : 0.5	Li : 0
O1	1.18	1.18	1.14	1.12	0.89	0.77	0.77	0.75	0.75
O2	1.02	1.02	1.03	0.88	0.88	0.81	0.66	0.64	0.67
O3	1.02	1.01	1.01	0.89	0.93	0.81	0.66	0.65	0.66
O4	1.11	1.09	1.09	1.05	0.95	0.88	0.74	0.73	0.74
O5	1.02	1.01	1.01	0.92	0.90	0.69	0.65	0.69	0.67
O6	1.02	1.02	1.04	0.97	0.91	0.69	0.65	0.65	0.67
O7	1.19	1.05	1.03	1.19	0.98	0.74	0.88	0.73	0.74
O8	1.10	1.09	1.04	0.97	0.93	0.76	0.66	0.66	0.66
O9	1.21	1.21	1.18	1.12	1.13	0.90	0.73	0.73	0.74
O10	1.03	1.02	1.00	1.00	0.82	0.68	0.66	0.63	0.65
O11	1.04	1.03	1.02	0.94	0.88	0.77	0.66	0.65	0.66
O12	1.06	1.06	1.04	0.94	0.95	0.80	0.63	0.62	0.65
O13	0.99	0.98	1.02	0.89	0.89	0.78	0.66	0.66	0.67
O14	1.20	1.20	1.19	1.14	0.90	0.75	0.74	0.72	0.75
O15	1.10	1.11	1.11	0.96	1.03	0.85	0.74	0.75	0.75
O16	1.07	1.08	1.07	0.92	0.91	0.80	0.67	0.66	0.67
O17	1.17	1.17	1.14	1.04	1.18	0.77	0.74	0.73	0.75
O18	1.20	1.20	1.18	1.17	0.97	0.79	0.73	0.74	0.74
O19	1.06	1.07	1.00	0.99	0.79	0.75	0.76	0.76	0.67
O20	1.19	1.17	1.16	1.04	0.97	0.89	0.73	0.72	0.75
O21	1.08	1.08	1.00	0.97	0.68	0.87	0.65	0.63	0.64
O22	1.08	1.09	1.07	0.98	0.95	0.73	0.63	0.63	0.65
O23	1.18	1.18	1.18	0.96	0.91	0.98	0.73	0.73	0.75
O24	1.06	1.06	0.94	0.94	0.94	0.78	0.77	0.77	0.64
O25	1.13	1.13	0.98	0.97	0.93	0.75	0.78	0.77	0.64
O26	1.08	1.08	1.09	1.02	0.96	0.65	0.63	0.63	0.65
O27	1.03	1.05	1.05	1.03	0.89	0.65	0.66	0.66	0.67
O28	1.04	1.04	1.01	1.05	0.88	0.67	0.66	0.64	0.64
O29	1.12	1.12	1.12	0.96	0.81	0.79	0.63	0.63	0.64
O30	1.02	1.01	0.90	0.95	0.85	0.74	0.79	0.73	0.65
O31	1.06	1.05	1.03	0.99	0.80	0.67	0.66	0.65	0.65
O32	1.11	1.12	1.11	0.98	0.77	0.65	0.62	0.65	0.65
O33	1.10	1.10	1.10	1.11	0.78	0.69	0.66	0.66	0.66
O34	1.14	1.15	1.09	1.05	0.91	0.72	0.79	0.73	0.74
O35	1.12	1.12	1.11	1.10	0.89	0.74	0.72	0.75	0.74
O36	1.04	1.04	1.04	1.03	0.84	0.69	0.66	0.66	0.66
O37	1.17	1.03	1.02	1.07	0.87	0.86	0.82	0.72	0.74
O38	1.08	1.08	1.07	1.08	0.89	0.67	0.66	0.69	0.67
O39	1.05	1.04	1.04	0.97	0.80	0.74	0.63	0.63	0.65
O40	1.14	1.11	1.13	1.03	1.03	0.88	0.72	0.72	0.74
O41	1.04	1.04	1.04	0.95	0.68	0.74	0.64	0.66	0.65
O42	1.01	0.94	0.98	1.00	0.81	0.66	0.76	0.65	0.67
O43	1.09	0.94	0.93	0.96	0.89	0.80	0.73	0.63	0.65
O44	1.06	1.06	1.03	0.93	0.96	0.79	0.64	0.63	0.65
O45	1.12	1.13	1.14	0.96	0.94	0.72	0.73	0.73	0.74
O46	1.10	1.10	0.97	0.96	0.82	0.76	0.76	0.66	0.66
O47	1.10	1.09	1.08	0.95	0.86	0.82	0.65	0.66	0.66
O48	1.13	1.06	1.06	1.01	1.09	0.83	0.84	0.72	0.74
O49	1.05	1.05	1.01	0.91	0.94	0.77	0.67	0.66	0.66
O50	1.11	1.11	1.04	0.99	0.93	0.93	0.84	0.72	0.74
O51	1.03	1.01	0.96	0.79	0.86	0.75	0.63	0.63	0.64
O52	0.99	0.99	0.91	0.79	0.77	0.76	0.78	0.67	0.67
O53	1.03	1.03	1.04	0.90	0.88	0.69	0.64	0.64	0.65
O54	1.11	1.11	1.11	0.99	0.88	0.89	0.73	0.72	0.75
O55	1.02	1.03	1.02	0.86	0.68	0.80	0.63	0.63	0.65
O56	1.06	1.06	1.07	0.85	0.89	0.76	0.63	0.62	0.65
O57	1.05	1.04	1.02	0.92	0.78	0.80	0.63	0.63	0.65
O58	1.11	1.10	1.05	0.94	0.77	0.66	0.65	0.64	0.64
O59	1.03	1.01	1.02	0.96	0.78	0.77	0.65	0.63	0.65
O60	1.07	1.07	0.94	0.93	0.75	0.76	0.73	0.72	0.64
O61	1.00	0.99	0.98	0.81	0.92	0.86	0.65	0.66	0.67
O62	1.11	1.10	1.10	1.02	0.90	0.75	0.78	0.72	0.75

O63	1.13	1.13	1.14	1.05	0.90	0.80	0.74	0.73	0.75
O64	1.04	0.92	0.92	0.91	0.76	0.80	0.75	0.77	0.67
O65	1.09	1.07	1.08	1.06	0.85	0.84	0.77	0.74	0.75
O66	1.12	1.12	1.08	1.01	0.83	0.86	0.73	0.73	0.74
O67	1.04	1.04	1.06	0.97	0.78	0.75	0.67	0.66	0.66
O68	1.13	1.04	1.07	1.06	0.92	0.82	0.83	0.89	0.74
O69	1.04	1.04	0.96	0.91	0.66	0.81	0.77	0.65	0.66
O70	1.09	0.95	0.95	0.98	0.78	0.81	0.75	0.75	0.64
O71	1.19	1.19	1.12	1.11	0.94	0.75	0.85	0.73	0.74
O72	1.04	1.04	1.06	0.92	0.77	0.84	0.64	0.63	0.65
O73	1.21	1.19	1.16	1.10	0.91	0.86	0.74	0.73	0.74
O74	1.04	1.05	1.06	0.92	0.91	0.76	0.66	0.65	0.66
O75	1.02	1.03	1.02	0.91	0.82	0.75	0.67	0.67	0.67
O76	1.16	1.12	1.10	1.06	0.97	0.86	0.73	0.73	0.75
O77	1.02	1.00	0.93	0.97	0.80	0.81	0.76	0.66	0.67
O78	1.09	0.99	1.01	0.94	0.80	0.75	0.77	0.65	0.66
O79	1.11	1.09	1.10	1.08	0.89	0.76	0.73	0.73	0.74
O80	1.05	1.06	1.00	0.91	0.96	0.79	0.78	0.66	0.67
O81	1.14	1.03	1.05	1.10	0.89	0.65	0.73	0.74	0.64
O82	1.04	1.02	0.92	0.98	0.81	0.80	0.73	0.63	0.65
O83	1.02	0.93	0.93	0.98	0.86	0.66	0.77	0.77	0.67
O84	1.11	1.11	1.12	0.93	0.93	0.73	0.65	0.62	0.65
O85	1.08	1.09	1.11	0.95	0.89	0.78	0.63	0.64	0.65
O86	1.08	1.08	0.98	0.94	0.67	0.80	0.78	0.62	0.64
O87	1.17	1.17	1.10	1.00	0.86	0.84	0.73	0.73	0.74
O88	1.03	1.03	1.04	0.85	0.83	0.75	0.64	0.64	0.64
O89	1.10	0.97	0.97	0.92	0.94	0.75	0.79	0.75	0.65
O90	1.06	1.06	1.03	0.89	0.75	0.75	0.63	0.62	0.64
O91	1.04	1.01	1.02	0.98	0.89	0.78	0.67	0.63	0.65
O92	1.00	1.00	0.99	0.93	0.87	0.79	0.64	0.63	0.65
O93	1.11	1.12	1.11	0.93	0.98	1.03	0.73	0.72	0.74
O94	1.07	1.05	1.06	1.01	0.95	0.77	0.68	0.67	0.67
O95	1.03	1.03	1.04	0.83	0.93	0.81	0.65	0.66	0.66
O96	1.19	1.19	1.19	0.93	1.01	0.97	0.73	0.72	0.74
O97	1.10	1.08	1.08	0.94	0.98	0.82	0.67	0.66	0.66
O98	1.11	1.04	1.04	1.02	0.88	0.85	0.83	0.82	0.74
O99	1.12	1.11	0.99	1.00	0.95	0.71	0.73	0.65	0.65
O100	1.07	0.96	0.97	0.94	0.80	0.78	0.76	0.77	0.66
O101	1.11	1.11	1.07	0.94	0.95	0.79	0.63	0.63	0.64
O102	1.18	1.18	1.16	1.01	0.99	0.95	0.73	0.72	0.74
O103	1.09	1.10	1.10	1.06	0.81	0.67	0.64	0.64	0.65
O104	1.10	0.96	0.96	0.90	0.81	0.84	0.76	0.74	0.65
O105	1.08	1.06	0.92	1.02	0.83	0.78	0.80	0.68	0.66
O106	1.18	1.18	1.18	1.20	0.87	0.74	0.74	0.74	0.75
O107	1.19	1.17	1.07	1.12	0.90	0.90	0.83	0.73	0.74
O108	1.05	1.04	1.02	0.87	0.83	0.79	0.65	0.67	0.66
O109	1.11	1.11	1.03	1.06	0.93	0.85	0.83	0.84	0.74
O110	1.04	1.03	1.02	1.04	0.79	0.69	0.66	0.66	0.67
O111	1.05	0.94	0.92	1.08	0.90	0.63	0.79	0.75	0.65
O112	1.15	1.15	1.15	1.14	0.97	0.79	0.74	0.74	0.75
O113	1.08	1.05	1.05	1.07	0.83	0.76	0.64	0.63	0.65
O114	1.02	1.02	0.99	1.01	0.81	0.69	0.70	0.66	0.68
O115	1.04	1.03	1.02	1.05	0.89	0.68	0.62	0.64	0.64
O116	1.01	1.02	1.03	1.04	0.92	0.72	0.63	0.63	0.65
O117	1.05	0.96	0.99	0.96	0.98	0.76	0.73	0.74	0.65
O118	1.09	1.09	1.08	0.97	0.90	0.93	0.63	0.63	0.65
O119	1.04	0.96	0.98	1.02	0.89	0.67	0.74	0.75	0.65
O120	1.11	1.10	1.08	1.09	0.96	0.63	0.63	0.62	0.65

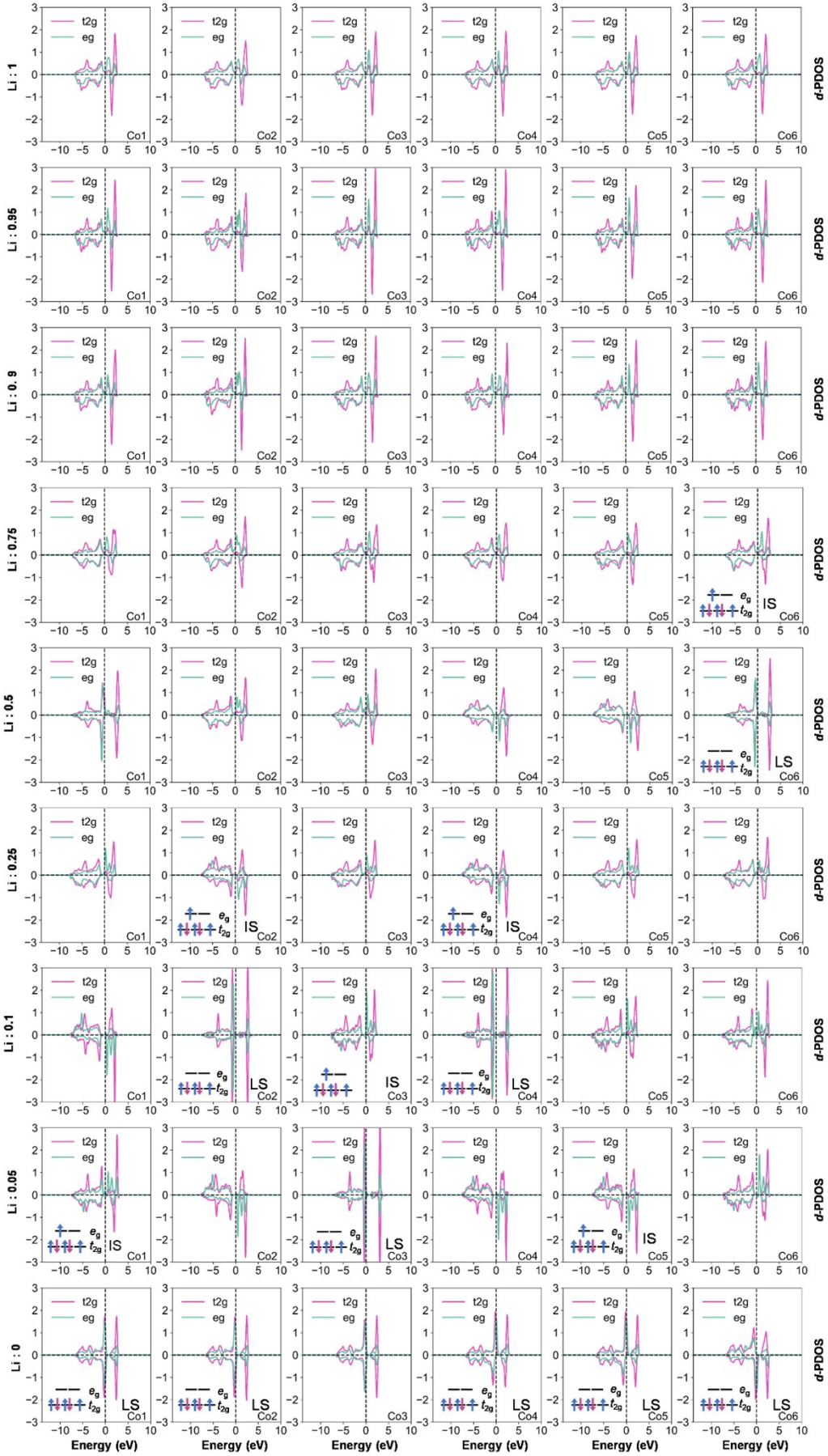

Fig. S6. Partial DOS of Co atoms and their spin configurations in structures with different lithium concentrations.

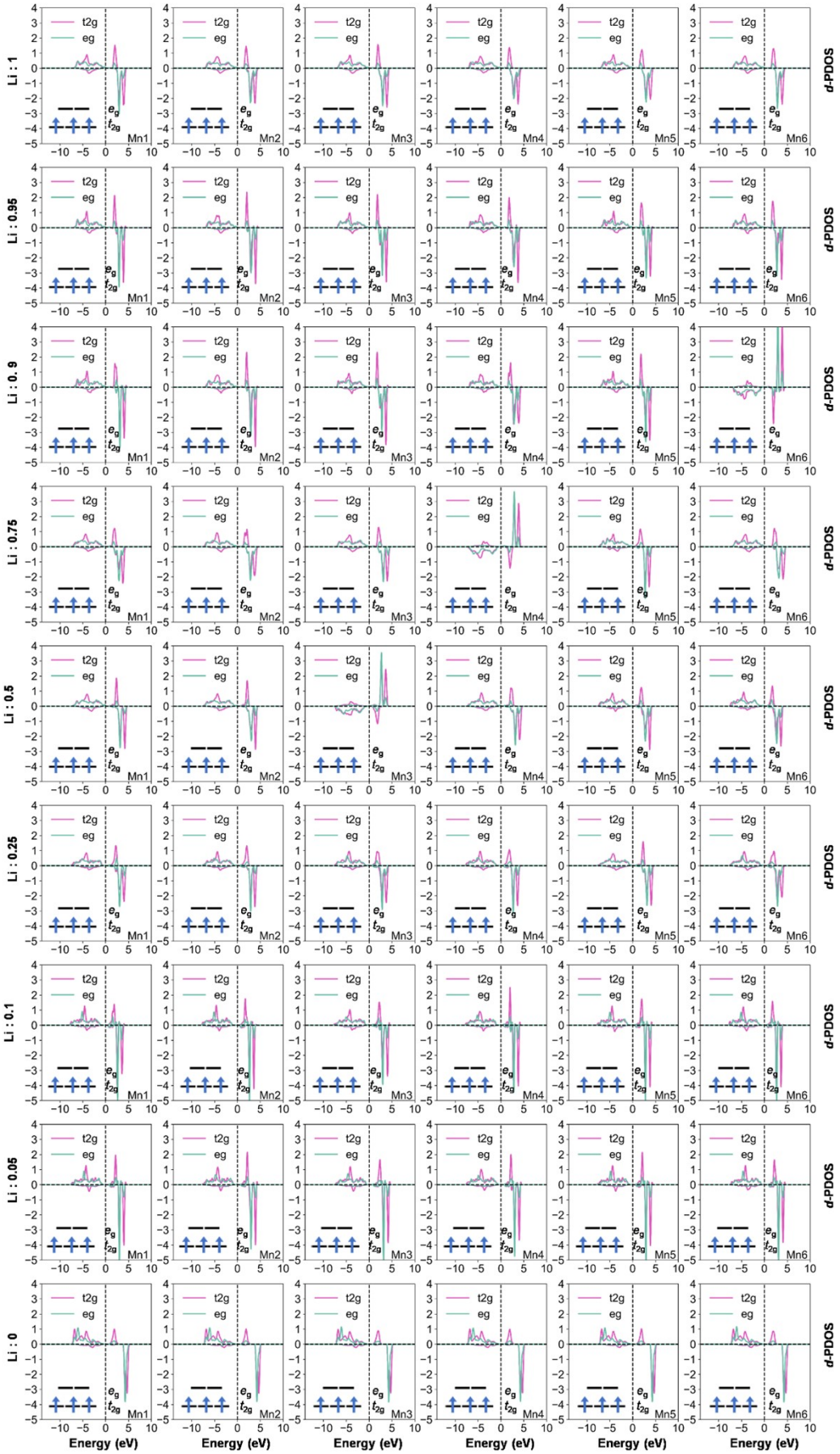

Fig. S7. Partial DOS of Mn atoms and their spin configurations in structures with different lithium concentrations.

Research for unequal trends in lattice parameters *a* and *b*

In the initial charging stage (SOC<10%), as shown in Fig. S7(a), the changing trends of lattice parameters a and b remain consistent, which can be attributed to the uniform distribution of Ni^{2+} participating in oxidation in the TM layer. When the SOC exceeds 25%, the lattice parameter *b* decreases drastically compared to the lattice parameter *a*. To investigate the reasons leading to the aforementioned results, the distributions of Ni^{4+} in the crystals with different lithium contents were labeled as shown in Fig. S7 (b-d). The Ni^{4+} produced by the oxidation reaction is not in the same straight line in the lattice a direction but in the lattice *b* direction, which will linearly reduce the value of the lattice *b*. Consequently, the shortened bond lengths and reduced ionic radii directly lead to a changing trend of the lattice parameter *b* inconsistent with that of the lattice parameter *a*.

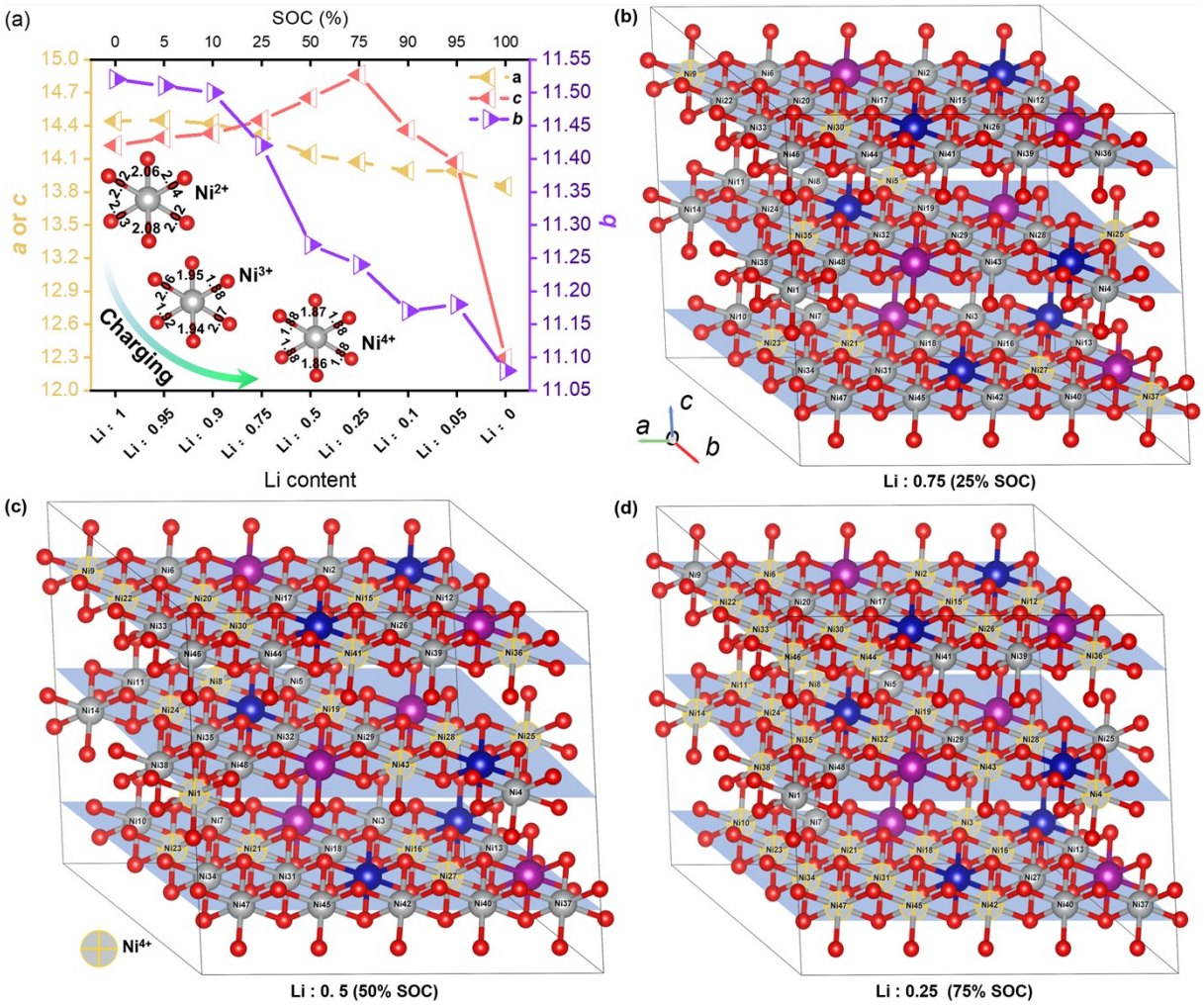

Fig. S8 (a) Calculated *a*-, *b*- and *c*-direction lattice parameters, and inset graph showing Ni-O bond length parameters with charging process. (b-d) Distribution of Ni^{4+} in the crystal structure with different Li contents. Li atoms are hidden to display the numbers corresponding to Ni atoms. Co is not labeled due to its small amount compared to Ni.

Reference

1. C. Xing, H. Da, P. Yang, J. Huang, M. Gan, J. Zhou, Y. Li, H. Zhang, B. Ge and L. Fei, *ACS Nano*, 2023, **17**, 3194.
2. H. Zhuo, H. Peng, B. Xiao, Z. Wang, X. Liu, Z. Li, G. Li, X. Bai, L. Wang, X. Huang, J. Wu, W. Quan, J. Wang, W. Zhuang and X. Sun, *Adv. Energy Mater.*, 2023, **13**, 2203354.
3. T. Liu, J. Liu, L. Li, L. Yu, J. Diao, T. Zhou, S. Li, A. Dai, W. Zhao, S. Xu, Y. Ren, L. Wang, T. Wu, R. Qi, Y. Xiao, J. Zheng, W. Cha, R. Harder, I. Robinson, J. Wen, J. Lu, F. Pan and K. Amine, *Nature*, 2022, **606**, 305.

4. X. Li, Q.-B. Liu, Y. Tang, W. Li, N. Ding, Z. Liu, H.-H. Fu, S. Dong, X. Li and J. Yang, *J. Am. Chem. Soc.*, 2023, **145**, 7869.
5. F. Rahmawati, B. Prijamboedi, S. Soepriyanto and Ismunandar, *Int. J. Miner. Metall. Mater.*, 2012, **19**, 863.
6. X. Lin, C. Li, K. Su and J. Ni, *Phys. Rev. B*, 2022, **106**, 075423.